High-transmittance in-plane-switching liquid-crystal displays using a positive-dielectric-anisotropy liquid crystal

Zhibing Ge
Xinyu Zhu
Thomas X. Wu
Shin-Tson Wu

Abstract — The in-plane-switching (IPS) mode exhibits an inherently wide viewing angle and has been widely used for liquid-crystal-display (LCD) TVs. However, its transmittance is limited to ~76% compared to that of a twisted-nematic (TN) cell if a positive-dielectric-anisotropy LC is employed. A special electrode configuration that fuses the switching mechanism of the conventional IPS and the fringe-field switching (FFS) to boost the transmittance to ~90% using a positive LC has been developed. The new mode exhibits an equally wide viewing angle as the IPS and FFS modes.

Keywords — *Liquid crystal, in-plane switching, fringe-field switching, high tramsmittance.*

1 Introduction

Large-screen LCD TV is emerging rapidly because of the integrated progress in wide viewing angle, fast response time, high contrast ratio, thin-film transistor (TFT), blinking backlight, and manufacturing technologies. To achieve wide viewing, film-compensated multi-domain in-plane switching (IPS) and multi-domain vertical alignment (MVA) are the two major approaches.[1] Both technologies have demonstrated high contrast ratio (>1000:1) and a viewing angle of almost 180°. However, there are still several technical challenges for perfecting LCD-TV performance. For instance, to enhance the LCD-panel light throughput in order to reduce the cost by eliminating the brightness-enhancement films, to improve the LC response time in order to reduce image blurring, to reduce the color shift at oblique angles, and to increase color saturation by using a light-emitting-diode (LED) backlight.

For the IPS-based technologies, two types of switching mechanisms have been developed: the conventional IPS mode[2,3] and the fringe-field switching (FFS) mode.[4–6] Both modes use initially homogeneous alignment driven by horizontal fields to achieve a wide viewing angle. A positive-dielectric-anisotropy ($\Delta\varepsilon$) LC is commonly employed in most IPS cells, while a negative $\Delta\varepsilon$ LC is preferred for the FFS cells. From a materials viewpoint, a positive $\Delta\varepsilon$ LC usually exhibits a larger $\Delta\varepsilon$ and lower viscosity than its negative counterpart, making it preferable for displays requiring low operating voltage and fast response. However, in conventional IPS cells, the electrode width and distance between the pixel and common electrodes are *larger* than the LC cell gap so that strong vertical electric fields are generated above the electrode surfaces. The LC directors there experience tilt rather than twist, if a positive $\Delta\varepsilon$ LC is employed, which leads to insufficient phase retardation. As a result, the overall light efficiency is only ~76% of that of a TN cell.[7] Using a negative $\Delta\varepsilon$ LC would enhance the light efficiency to ~86%, but the tradeoff is the increased driving voltage which, in turn, increases power consumption.

To improve light efficiency, the FFS mode using a positive $\Delta\varepsilon$ LC was proposed.[6] Different from the conventional IPS mode, the FFS mode requires the electrode width and the distance between pixel and common electrodes to be *smaller than* the LC cell gap in order to generate sufficiently strong fringe fields with both horizontal and vertical components to reorient the LC directors in the center of the electrodes. When using a positive $\Delta\varepsilon$ LC in the FFS mode, the light efficiency can reach 90% if the electrode width is ~1 μm.[6] However, to obtain high manufacturing yield, the current TFT photolithographic process is commonly practiced at no less than a 3-μm resolution. Further optimization for the FFS mode using a positive $\Delta\varepsilon$ LC material is still under active research.

In this paper, we demonstrate two new electrode designs to improve the transmittance of conventional IPS LCD panels. In our high-transmittance IPS (HT-IPS) mode, using a positive $\Delta\varepsilon$ LC the electrode width and gap are intentionally kept *equal* to or *larger* than 3 μm for the consideration of high yield manufacturing. The switching mechanism and performance, such as voltage-dependent transmittance, iso-brightness, iso-contrast, and response time of the HT-IPS, are investigated and the results are compared to those of the IPS and FFS modes.

2 Cell design and mechanism

Figures 1(a) and 1(b) depict the typical cell structures (lower part) and the simulated on-state LC director distributions with equal potential lines (upper part) of a conventional IPS cell and a FFS cell, respectively. In the IPS cell, the electrode width w and the horizontal distance l between adjacent pixel and common electrodes are usually kept *larger* than the cell gap d. Under such a configuration, sub-

Z. Ge and T. X. Wu are with the School of Engineering and Computer Science, University of Central Florida, P.O. Box 162700, Orlando, FL 32816, U.S.A.; telephone 407/823-3524, e-mail: zge@creol.ucf.edu.

X. Zhu and S-T. Wu are with the College of Optics and Photonics, University of Central Florida, Orlando, FL, U.S.A.

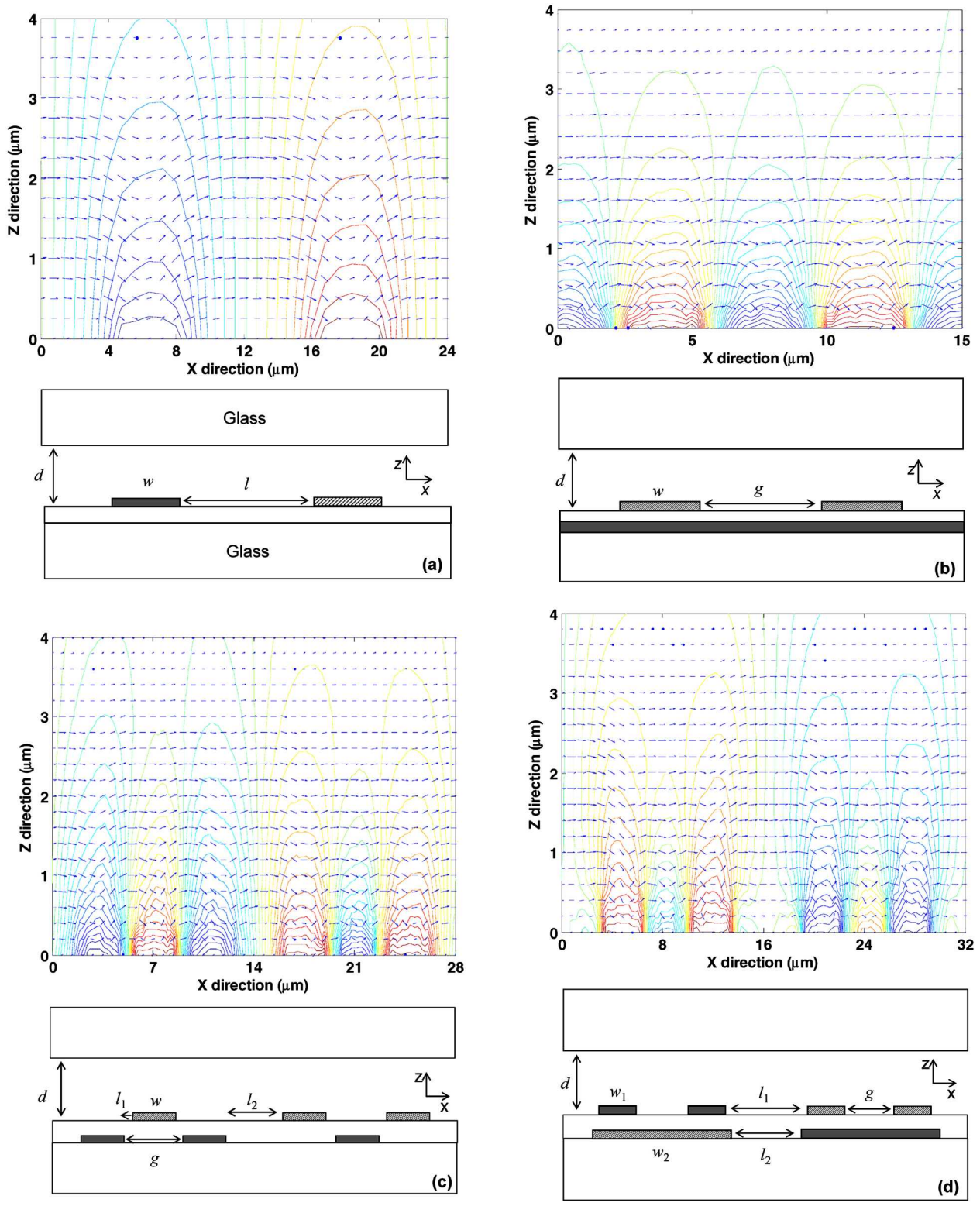

FIGURE 1 — Structures and director profiles with equal potential lines of the (a) IPS, (b) FFS, (c) HT-IPS-1, and (d) HT-IPS-2 cell using a positive Δε LC material.

stantial horizontal electric fields exist only between the electrodes, which effectively twist the LC directors in this region. However, above the electrode surface the horizontal field is weak and the vertical field is strong, which tilts rather than twists the LC directors. Consequently, the light efficiency in an IPS cell is reduced.

As for the FFS cell shown in Fig. 1(b), both electrode width w and horizontal distance (l = 0 in this case, as referred

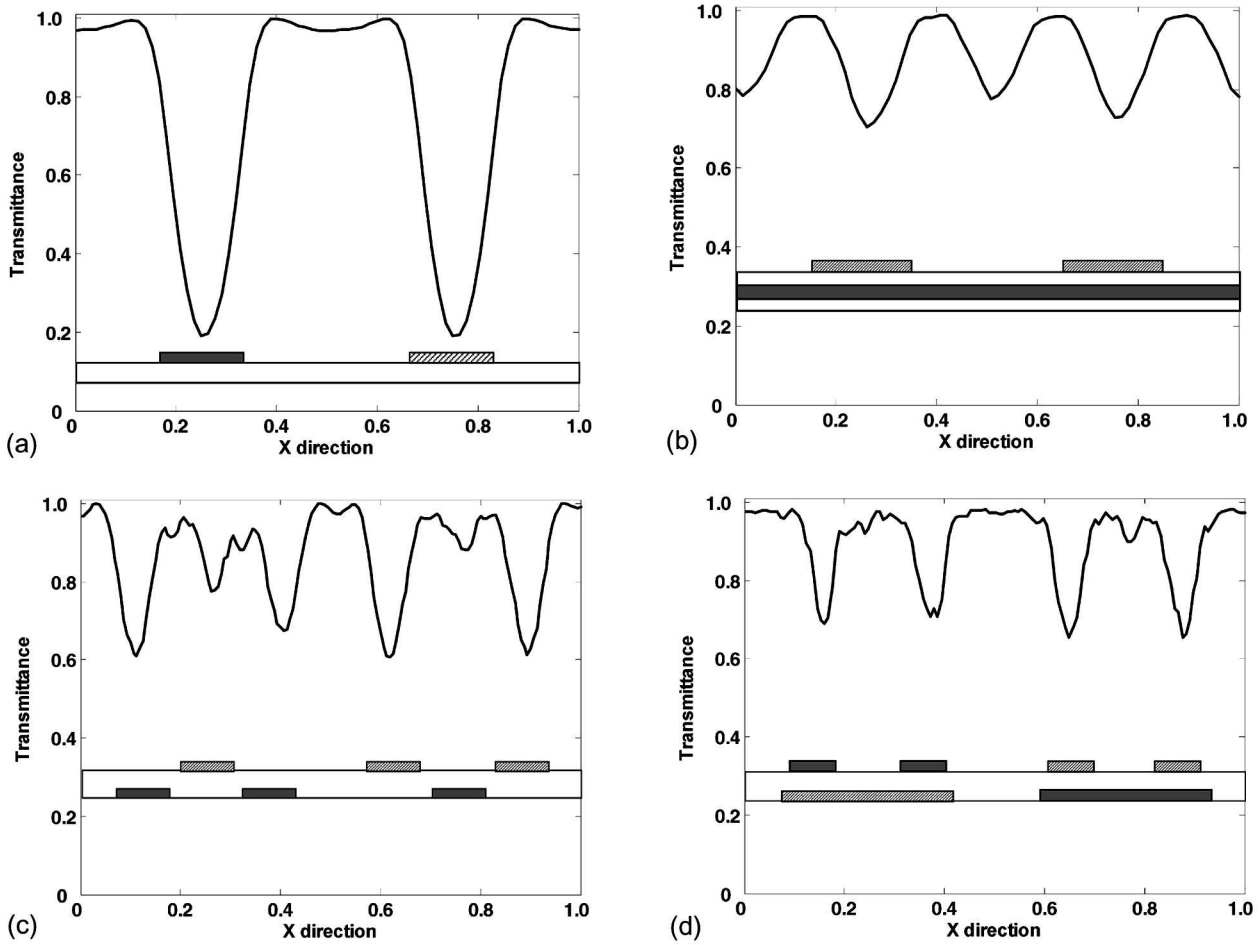

FIGURE 2 — Transmittance curves with respect to electrode position of the (a) IPS, (b) FFS, (c) HT-IPS-1, and (d) HT-IPS-2 cell.

to the IPS structure; this distance is not the electrode gap g) between the pixel electrode and the bottom common electrode are *smaller* than the cell gap d. With decreased dimensions, the fringe fields possess both horizontal and vertical components throughout the whole cell. Moreover, the horizontal fields are the strongest at the electrode edges, but become the weakest at the symmetric centers above the electrodes and above the slits. Under such a field profile, the LC directors near the electrode edges will be the first rotated. Because of the small electrode width w and gap g, the twist of the LC directors near the edges can further rouse the directors in the left regions to twist, although the horizontal fields there are weak. As a result, the overall light efficiency for a FFS cell using a positive $\Delta\varepsilon$ LC material can be greatly enhanced, as compared to the IPS mode. However, because of the existence of vertical electric-field components in the symmetric centers above the electrodes and the slits, positive $\Delta\varepsilon$ LC directors still experience tilt in these regions, which needs further cell optimization.

In the HT-IPS designs shown in Figs. 1(c) (designated as HT-IPS-1) and 1(d) (HT-IPS-2), the electrodes are divided into two repetitive groups, *i.e.*, two common electrodes and one pixel electrode at one side form the first electrode group, where the overall potential is similar to a common electrode in the IPS cell; and two pixel electrodes with one common electrode at the other side form the second pixel-potential-like electrode group. The motivation is to gener-

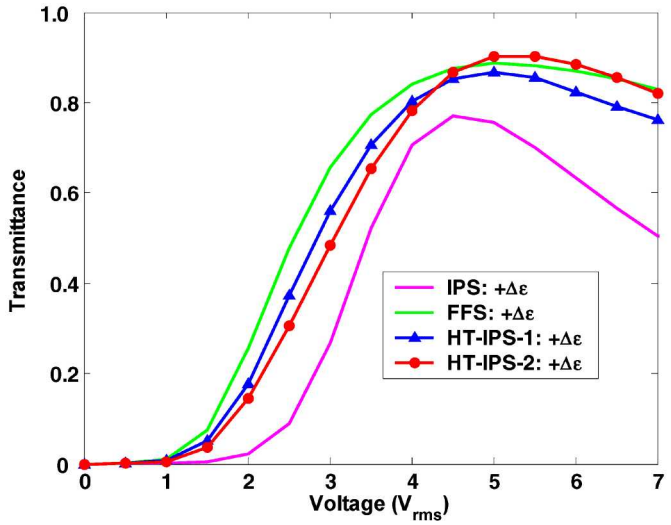

FIGURE 3 — V–T curves of the IPS, FFS, and HT-IPS cells using a $+\Delta\varepsilon$ LC material.

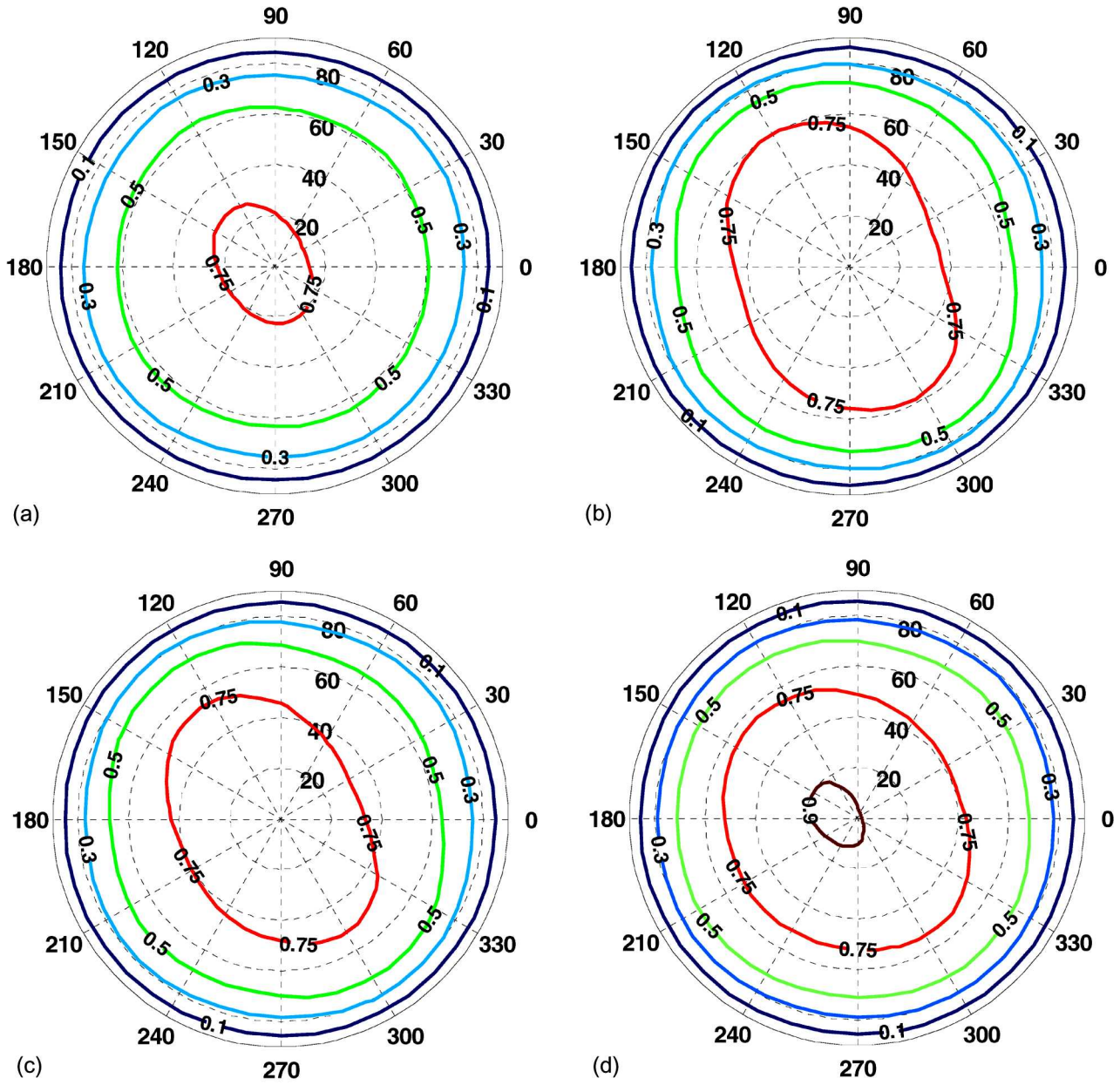

FIGURE 4 — Iso-brightness plots at T = 75%, 50%, 30%, and 10% of the (a) IPS, (b) FFS, (c) HT-IPS-1, and (d) HT-IPS-2 cell using a positive $\Delta\varepsilon$ LC material.

ate a region with substantial horizontal fields between electrode groups, similar to the conventional IPS mode, but introduce fringe fields with more horizontal electric-field components only in the regions above electrodes as the FFS mode.

In order to achieve the above-mentioned field profile, within each subgroup, the electrode width and horizontal distance between pixel and common electrodes are set *smaller* than the cell gap d, *i.e.*, w and l_1 in Fig. 1(c) and w_1 in Fig. 1(d) are kept *smaller* than d. Therefore, much richer horizontal electric fields combined with the vertical components are generated within each electrode group than they are in the regions above the electrode surfaces in the conventional IPS cell. However, to maintain the substantial horizontal electric fields generated between different electrode groups just as in the regions between electrodes in the IPS mode, the distance between adjacent electrodes from two electrode groups, such as the distance l_2 in Fig. 1(c), and l_1 and l_2 in Fig. 1(d) are kept *equal* to or *larger* than the cell gap d. The characteristics of this desired electric-field distribution can clearly be verified by the calculated potential profiles shown in Figs. 1(c) and 1(d). When a voltage above the threshold value is applied on the electrodes, the LC directors within each electrode group can be rotated by fringe fields and those between the electrode groups can be rotated by the strong horizontal fields there. Consequently, the overall light efficiency can be improved.

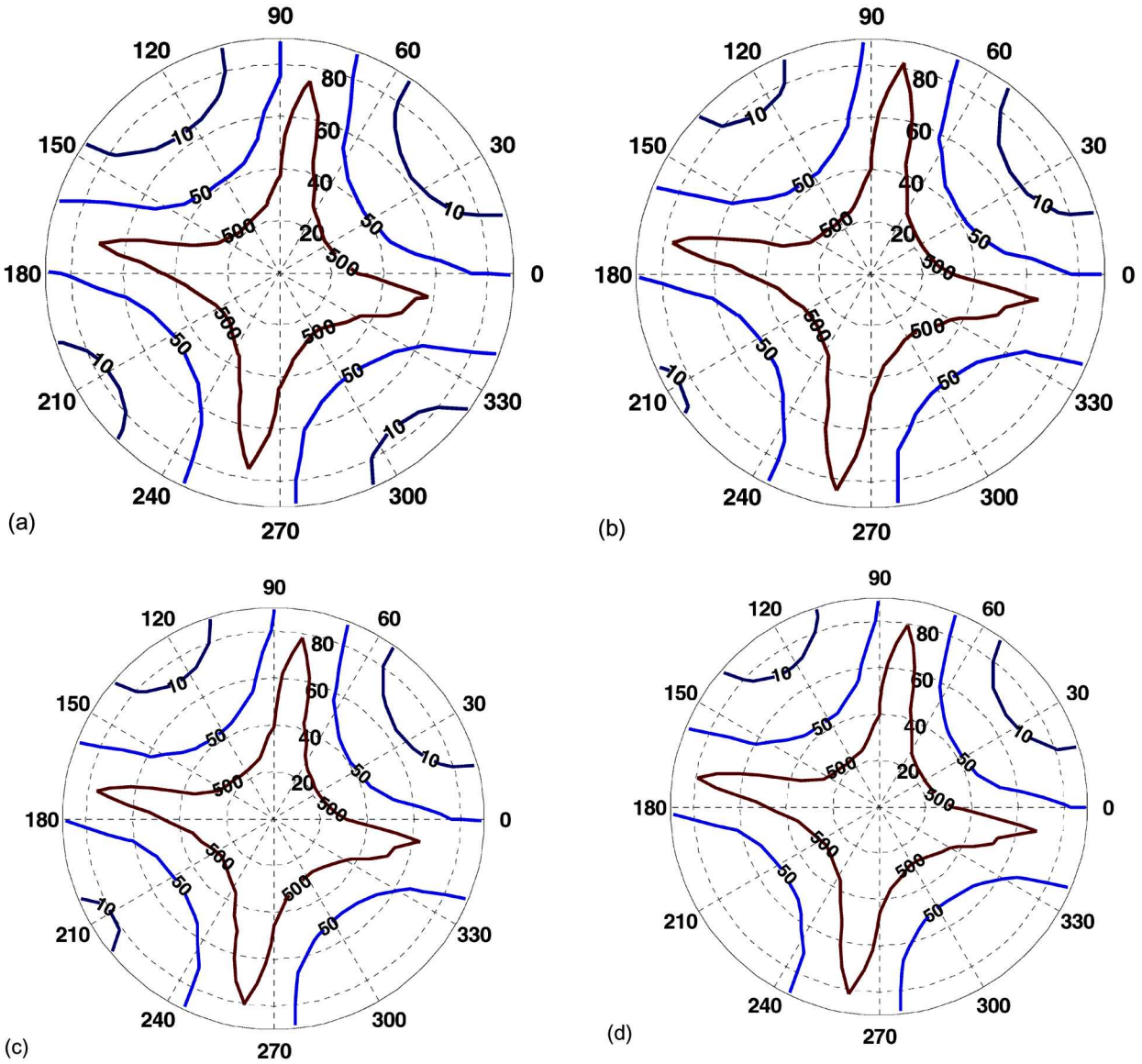

FIGURE 5 — Iso-contrast plots at CR = 500, 100, and 10 of the (a) IPS, (b) FFS, (c) HT-IPS-1, and (d) HT-IPS-2 cell using a positive Δε LC material.

3 Results and discussion

The electro-optic (EO) performance of the HT-IPS mode using a positive Δε LC material (MLC-6686 from Merck: dielectric anisotropy Δε = 10.0, K_{11} = 8.8 pN, K_{33} = 14.6 pN, and optical birefringence Δn = 0.095 at λ = 589 nm) is studied by the commercial LCD simulator 2dimMOS®.[8] The conventional IPS cell and the FFS are also studied as benchmarks for comparison. The present state-of-the-art TFT manufacturing process prefers a photolithographic feature size no less than 3 μm.[6] For the IPS cell, its cell parameters are kept at its typical values with w = 4 μm and l = 8 μm, and typical FFS electrode dimensions are w = 3 μm and g = 4.5 μm. In the HT-IPS cell in Fig. 1(c), w = 3 μm, g = 4 μm, and l_2 = 4 μm, while in the cell in Fig. 1(d), w_1 = 3 μm, w_2 = 11 μm, g = 4 μm, l_1 = 5 μm, and l_2 = 6 μm. And the cell gap d is kept at 4 μm in all these cells. The light efficiency is calculated by the extended Jones matrix method.[9]

Figures 2(a) to 2(d) show the normalized transmittance with respect to the position in a single electrode period for the conventional IPS cell in Fig. 1(a), the FFS cell in Fig. 1(b), and the HT-IPS cells in Figs. 1(c) and 1(d), respectively. The corresponding electrode position is normalized to the period and included in these figures as a reference. Accordingly, the averaged light efficiency for these cells using a positive Δε material is around 76, 88, 87, and 90% of that of a TN cell. The HT-IPS structure in Fig. 1(d) shows the highest transmittance which is slightly better than the FFS cell because the electric fields within and between the electrode groups can switch the LC directors more efficiently. A drawback is the increased electrode complexity. The low transmittance kinks in these cells come from the tilt

TABLE 1 — Summary of IPS, FFS, and HT-IPS cells using a positive Δε LC material.

	Transmittance (%)	V_{th}/V_{on} (V_{rms})	τ_{on}/τ_{off} (msec)	Features
IPS	76	1.5/4.5	29/29	▪ $w, l \geq d$ ▪ Strong vertical fields existing above electrode surface; and substantial horizontal fields existing between electrodes.
FFS	88	1.0/5.0	27/29	▪ $w, l \leq d$ ▪ Fringe fields with both vertical and horizontal components existing throughout the entire cell.
HT-IPS-1	87	1.0/5.0	26/29	▪ $w, l_1 \leq d\,; l_2 \geq d$ ▪ Fringe fields existing within electrode group, and substantial horizontal fields existing between electrode groups.
HT-IPS-2	90	1.0/5.2	28/29	▪ $w_1 \leq d\,; l_1, l_2 \geq d$ ▪ Fringe fields existing within electrode group, and substantial horizontal fields existing between electrode groups.

of LC directors there, which mainly occur in the regions where vertical electric fields dominate as explained in Section 2. The overall light efficiency can be further improved, if the electrode width is further reduced.

Figure 3 depicts the voltage-dependent transmittance curves for the cells shown in Figs. 1(a) to 1(d). The IPS mode has the lowest transmittance because of the insufficient twist above the electrode surface, while the transmittance in the FFS cell and the HT-IPS cells are greatly enhanced. Furthermore, because the IPS cell has the largest *l/d* ratio, it shows the highest threshold voltage ($V_{th} \sim 1.5V_{rms}$) as compared to that of the FFS and HT-IPS cells ($V_{th} \sim 1.0V_{rms}$). However, the transmittance of the IPS cell reaches its maximum at $\sim 4.5V_{rms}$, while it saturates at $\sim 5.0V_{rms}$ in the FFS cell and the HT-IPS cells. In the IPS cell with the current cell gap, its overall transmittance is primarily contributed from the regions between electrodes, where the LC directors are easily rotated by the horizontal fields there; and the regions above electrode surfaces make a limited contribution because the LC directors there mainly tilt, rather than twist. Once the transmittance saturates, a further increase in the voltage will over-twist the directors between the electrodes, resulting in a decrease of the overall transmittance. However, in the FFS cell and the HT-IPS cells, the entire cell region contributes to the overall light efficiency. As the voltage increases, the horizontal fields rotate the LC directors near the electrode edges first and then extend to the neighborhood and, finally, to the center of the electrodes. This process makes the transmittance saturate at a higher voltage than the IPS cell.

The improvement of transmittance in the normal direction also helps to enhance the iso-brightness performance. The iso-brightness plots for the IPS, FFS, and HT-IPS cells are shown in Figs. 4(a)–4(d), respectively. As shown in Fig. 4(a), the $T \geq 75\%$ cone in the IPS cell is confined within a polar angle of 20° at most azimuthal directions. Because of the increased LC director rotation throughout the entire cell, the viewing cones are greatly enhanced in the FFS cell and the HT-IPS cells. The $T \geq 75\%$ viewing cones in these three cells are expanded to above 40° and even above 55° at some directions in Figs. 4(b)–4(d). Moreover, the HT-IPS cell in Fig. 4(d) even exhibits a $T \geq 90\%$ viewing cone.

All these structures have the same initial homogeneous state and are driven by the in-plane fields, resulting in a same dark state. In other words, their on-state iso-brightness performance determines their corresponding iso-contrast plots. Figures 5(a)–5(d) show the iso-contrast plots for the above-mentioned structures. Without compensation films, the CR ≥ 10:1 viewing cone is also improved from IPS to HT-IPS cells. And the HT-IPS cell in Fig. 5(d) has a slightly better viewing angle than the IPS cell and the FFS cell. For TV applications, a wide viewing angle in LCD is critical. Various film compensation schemes of IPS and FFS modes have been developed.[10–12] The film compensation of the HT-IPS mode is similar to those of IPS and FFS modes.

The response times of these modes are also investigated with results listed in Table 1. The optical rise time (τ_{on}) and decay time (τ_{off}) are defined as transmittance rising from 10% to 90% and decaying from 90% to 10%, respectively. Because of the same cell gap and LC material employed, the response times of these modes are rather similar. It is known that response time can be shortened by using a thinner cell gap, lower viscosity LC mixture, elevated temperature operation, or applying overdrive and undershoot voltages.[13,14] Besides the response time, Table 1 also summarizes the major cell features and electro-optic properties of these four modes.

As the TFT fabrication technology continues to advance, the 2-μm and even 1-μm photolithographic processes may be feasible in the near future. Reducing electrode width to 2 μm or 1 μm will further reduce the tilt above the electrode surfaces and enhance the overall light efficiency. Besides, using a negative Δε LC material can also help to suppress the tilt in enhancing the transmittance.[15,16] A tradeoff is in the increased response time and threshold voltage because of the higher viscosity and smaller Δε of the negative LC materials.

4 Conclusion

The proposed HT-IPS LCD having a special electrode configuration can achieve ~90% transmittance within present 3-μm TFT photolithographic process. By properly designing the electrodes to generate substantial horizontal electric fields between electrode groups and fringe fields with rich horizontal components within electrode groups, the LC directors throughout the whole cell can be twisted. The electro-optic characteristics of the HT-IPS mode, such as voltage-transmittance curve, iso-brightness, and iso-contrast are superior to those of the conventional IPS and, slightly better than those of the FFS modes.

Acknowledgment

The authors are indebted to Toppoly Optoelectronics (Taiwan) for their financial support.

References

1 S T Wu and D K Yang, *Reflective Liquid Crystal Displays* (Wiley, New York, 2001).
2 R A Soref, "Field effects in nematic liquid crystals obtained with interdigital electrodes," *J Appl Phys* **45**, 5466–5468 (1974).
3 M Oh-e and K Kondo, "Electro-optical characteristics and switching behavior of the in-plane switching mode," *Appl Phys Lett* **67**, 3895–3897 (1995).
4 S H Lee, S L Lee, and H Y Kim, "Electro-optic characteristics and switching principle of a nematic liquid crystal cell controlled by fringe-field switching," *Appl Phys Lett* **73**, 2881–2883 (1998).
5 S H Lee, S M Lee, H Y Kim, J M Kim, S H Hong, Y H Jeong, C H Park, Y J Choi, J Y Lee, J W Koh, and H S Park, "Ultra-FFS TFT-LCD with super image quality and fast response time," *SID Symposium Digest Tech Papers* **32**, 485–487 (2001).
6 Y M Jeon, I S Song, S H Lee, H Y Kim, S Y Kim, and Y J Lim, "Optimized electrode design to improve transmittance in the fringe-field switching (FFS) liquid-crystal cell," *SID Symposium Digest Tech Papers* **36**, 328–331 (2005).
7 M Schadt and W Helfrich, "Voltage-dependent optical activity of a twisted-nematic liquid crystal," *Appl Phys Lett* **18**, 127–128 (1971).
8 Autronic-Melchers GmbH, available: http://www.autronic-melchers.com/.
9 A Lien, "Extended Jones matrix representation for the twisted nematic liquid-crystal display at oblique incidence," *Appl Phys Lett* **57**, 2767–2769 (1990).
10 Y Saitoh, S Kimura, K Kusafuka, and H Shimizu, "Optimum film compensation of viewing angle of contrast in in-plane-switching-mode liquid-crystal display," *Jpn J Appl Phys* **37**, 822–4828 (1998).
11 J E Anderson and P J Bos, "Methods and concerns of compensating in-plane-switching liquid crystal displays," *Jpn J Appl Phys* **39**, 6388–6392 (2000).
12 X Zhu, Z Ge, and S T Wu, "Analytical solutions for uniaxial-film-compensated wide-view liquid crystal displays," *J Display Technology* **2**, 2–20 (2006).
13 S T Wu, "Nematic liquid crystal modulator with response time less than 100 μsec at room temperature," *Appl Phys Lett* **57**, 986–988 (1990).
14 H Okumura and H Fujiwara, "A new low-image-lag drive method for large-size LCTVs," *SID Symposium Digest Tech Papers* **23**, 601–604 (1992).
15 Z Ge, X Zhu, S T Wu, and T X Wu, "High transmittance and wide viewing angle liquid-crystal display devices," U.S. Patent Application Pending (2005).
16 Z Ge, X Zhu, T X Wu, and S T Wu, "High transmittance in-plane switching liquid crystal displays," *J Display Technology* **2**, 114–120 (2006).

Zhibing Ge is a Ph.D. candidate at the School of Electrical Engineering and Computer Science, University of Central Florida (UCF), Orlando. His Ph.D. study focuses on modeling of liquid-crystal displays and photonic devices. He is a recipient of IEEE Laser and Electro-Optics Society Graduate Fellowship Award in 2006. Currently, he is serving as the chairman of the SID UCF student branch.

Xinyu Zhu received his Ph.D. degree from Changchun Institute of Optics, Fine Mechanics and Physics, Chinese Academy of Sciences, China, in 2001 and his B.S. degree from Jilin University, China, in 1996. He joined the College of Optics and Photonics, UCF as a research scientist in 2001. His currently research interests include reflective and transflective liquid-crystal displays, liquid-crystal–on–silicon (LCoS) projection display, wide-viewing-angle liquid-crystal displays and adaptive optics application with nematic liquid crystals.

Thomas X. Wu received his B.S.E.E. and M.S.E.E. degrees from the University of Science and Technology of China (USTC), Anhui, China, in 1988 and 1991, respectively, and the M.S. and Ph.D. degrees in electrical engineering from the University of Pennsylvania, Philadelphia, in 1997 and 1999, respectively. He is currently an associate professor at the School of Electrical Engineering and Computer Science, UCF, Orlando. His current research interests and projects include complex media, liquid-crystal devices, electronic packaging of RF SAW devices, electrical machinery, magnetics and EMC/EMI in power electronics, chaotic electromagnetics, millimeter-wave circuits, and CMOS/BiCMOS RFICs. He received the Distinguished Researcher Award from the College of Engineering and Computer Science, UCF, in April 2004. He is listed in *Who's Who in Science and Engineering, Who's Who in America,* and *Who's Who in the World.*

Shin-Tson Wu received his Ph.D. degree from the University of Southern California, Los Angeles. He is currently a PREP professor at College of Optics and Photonics, UCF, Orlando. His studies at UCF focus on liquid-crystal displays and liquid-crystal materials, bio-inspired photonics, and laser-beam steering. He has co-authored four books, *Fundamentals of Liquid Crystal Devices* (Wiley, 2006), *Introduction to Microdisplays* (Wiley, 2006), *Reflective Liquid Crystal Displays* (Wiley, 2001) and *Optics and Nonlinear Optics of Liquid Crystals* (World Scientific, 1993), four book chapters, over 350 papers, and 55 issued and pending patents. He is a Fellow of the IEEE, SID, and OSA.